

Paul Chery¹, Kyle Miller², Evan Miller³ and Eric Jankowski³
¹Macalester College, ²University of Puget Sound, ³Boise State University

Introduction

Organic solar cells are advantageous because they can be processed cost and energy efficiently out of abundant materials and roll-to-roll printed onto flexible substrates. However, they currently suffer from low efficiency¹.

The goal of this research is to understand the effect of temperature, solvent quality, solvent amount, and concentrations of organic photovoltaic (OPV) components on active layer morphology. This morphology is critical to device efficiency because it impacts the mobility of charge carriers through the active layer to the electrodes¹ (see Figure 1).

We use HOOMD-blue³, a particle simulation Python package including molecular dynamics, to simulate P3HT:PCBM blends (PC₆₁BM and PC₇₁BM) on a supercomputing cluster. We run simulations of several hundred molecules for up to 48 hours at a time.

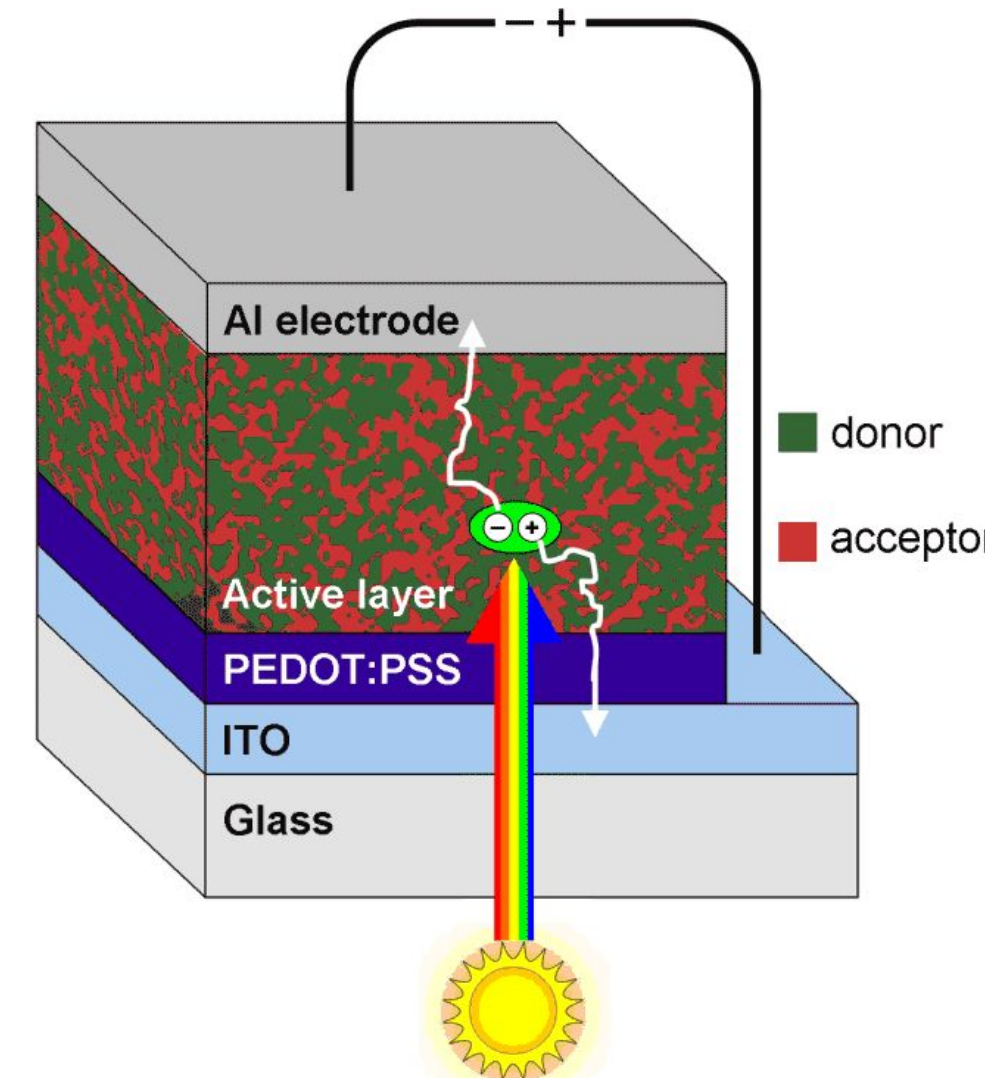


Figure 1: Schematic diagram of a bulk-heterojunction organic photovoltaic device². The P3HT acts as the donor and the PCBM as the acceptor material.

Molecular Model

We use a united-atom model and rigid bodies to simulate the molecules in our systems. The P3HT model is a 15-mer with the thiophene rings (rings of blue and orange atoms in Figure 2) treated as rigid bodies. The PC₆₁BM molecule is approximated by two rigid bodies, one for the buckyball and one for the benzene ring, while the PC₇₁BM is made up of one rigid body containing the bucky ball and benzene ring.

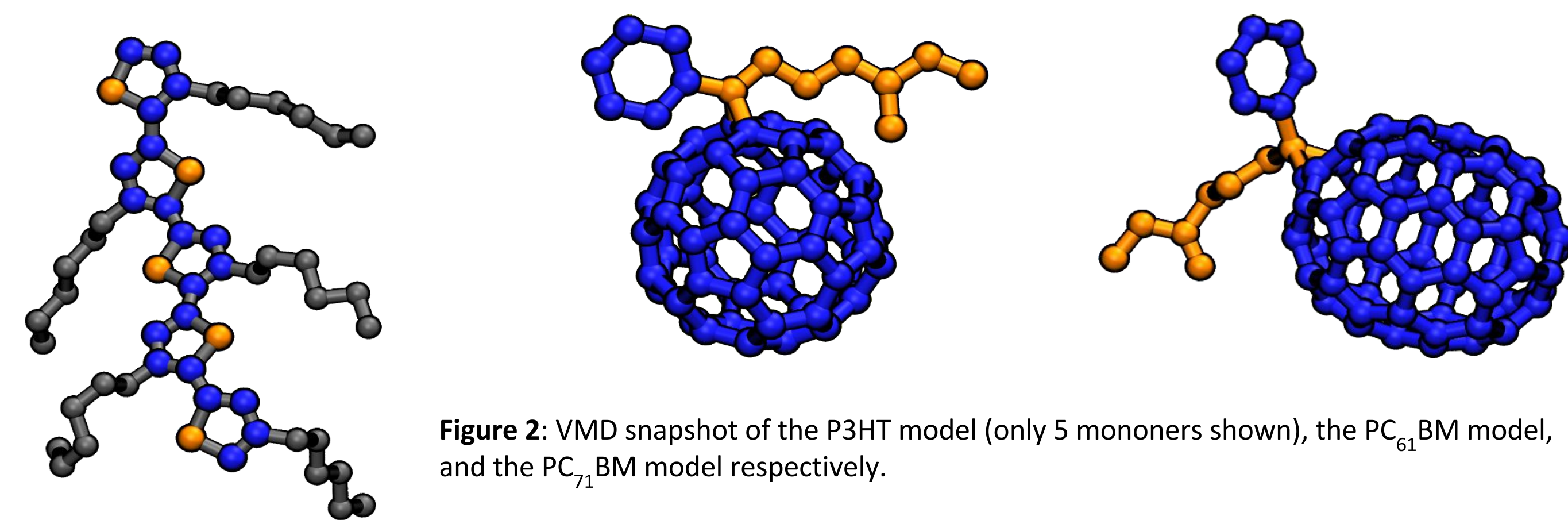


Figure 2: VMD snapshot of the P3HT model (only 5 monomers shown), the PC₆₁BM model, and the PC₇₁BM model respectively.

We use the Optimized Potential for Liquid Simulation for United Atom (OPLS-UA) force field to approximate the bonded, non-bonded, angle, and dihedral interactions within and between molecules. Our σ is 3.905 Å as prescribed by OPLS-UA.

Morphology Characterization

In order to characterize the morphology of our systems, we use the following tools:

- **Visual Molecular Dynamics (VMD)**: molecular visualization program useful for naked-eye observations and rough measurements of structure
- **Clustering algorithm**: calculates and allows visualization of molecular aggregation
- **Radial distribution function (RDF)**: calculates the occurrence of inter-structure distances, peaks in the graph correspond to distances with high probability.
- **Simulated grazing incidence X-ray scattering (GIXS) patterns**: help reveal the characteristic length scales and directionality of periodic features in a morphology
- **Structure factor**: radial average of a GIXS pattern that, like the RDF, yields characteristic length scales of a morphology, but in frequency space rather than coordinate space
- **Potential Energy**: a flat potential energy over time can indicate system equilibration, a downward trend indicates movement toward more energy minimizing configurations
- **P3HT end-to-end distance**: provides information about the shape of the oligomers which can affect their ability to π -stack

Results - P3HT:PCBM Blend

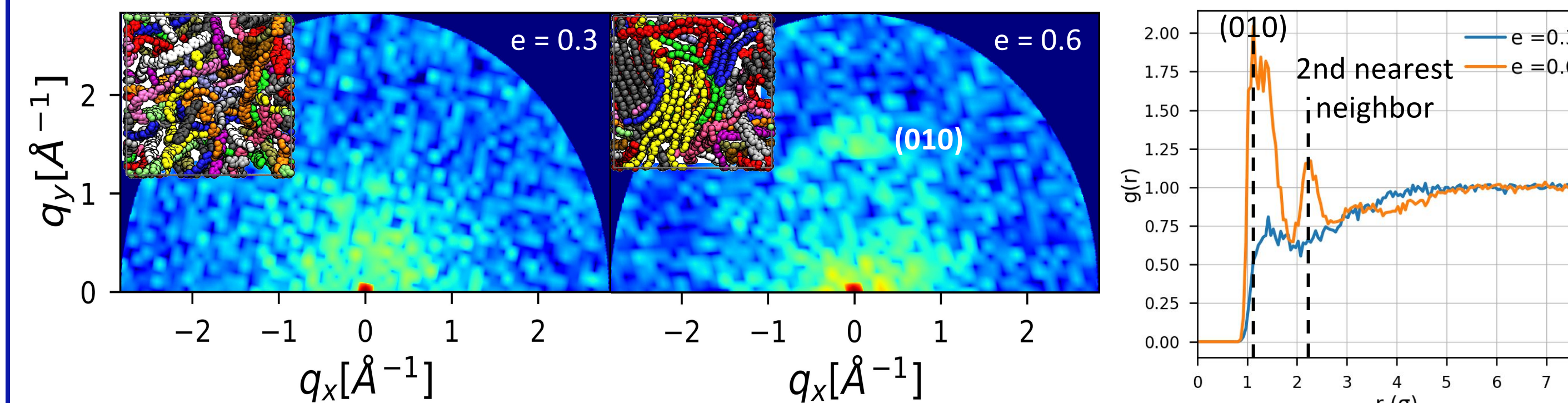


Figure 3: VMD snapshots (clustered) and simulated GIXS patterns of 1:1 PC₇₁BM system at T = 3.0, $\phi = 1.1$ (sys-A). (Left) Disordered with e = 0.3. (Right) Semi-ordered with e = 0.6.

The phase transition is evident above in the appearance of the (010) peak representing the distance between neighboring P3HT oligomers within a stack. A second nearest neighbor peak is also visible in Figure 4.

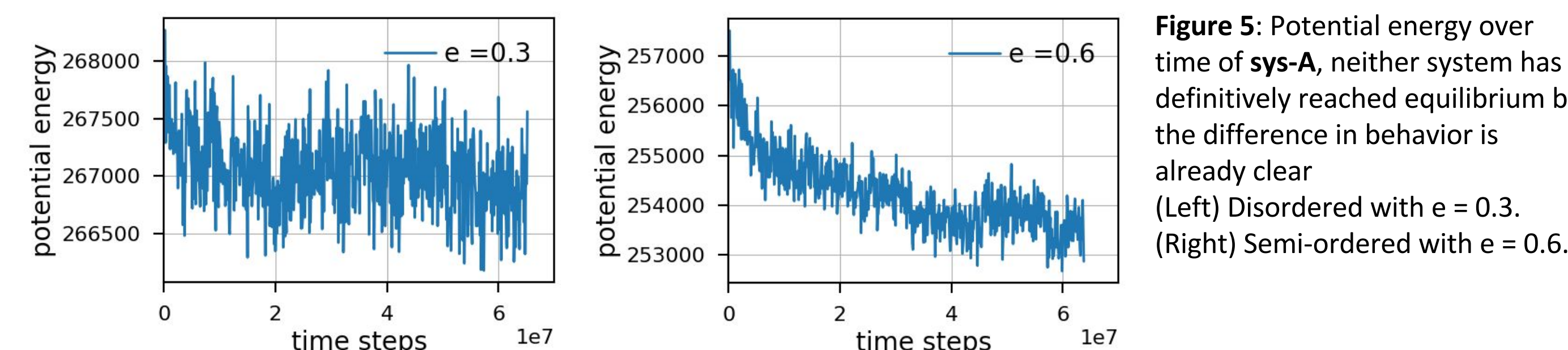


Figure 4: RDF (intra-oligomer exclusion) for sys-A.

The potential energy in the disordered system decreases by only 0.2% compared to 1.2% in the semi-ordered system since the system that self-assembles is progressing into a lower energy π -stacked morphology whereas the disordered system has an implicit solvent strong enough to dissolve the P3HT and prevent π -stacking.

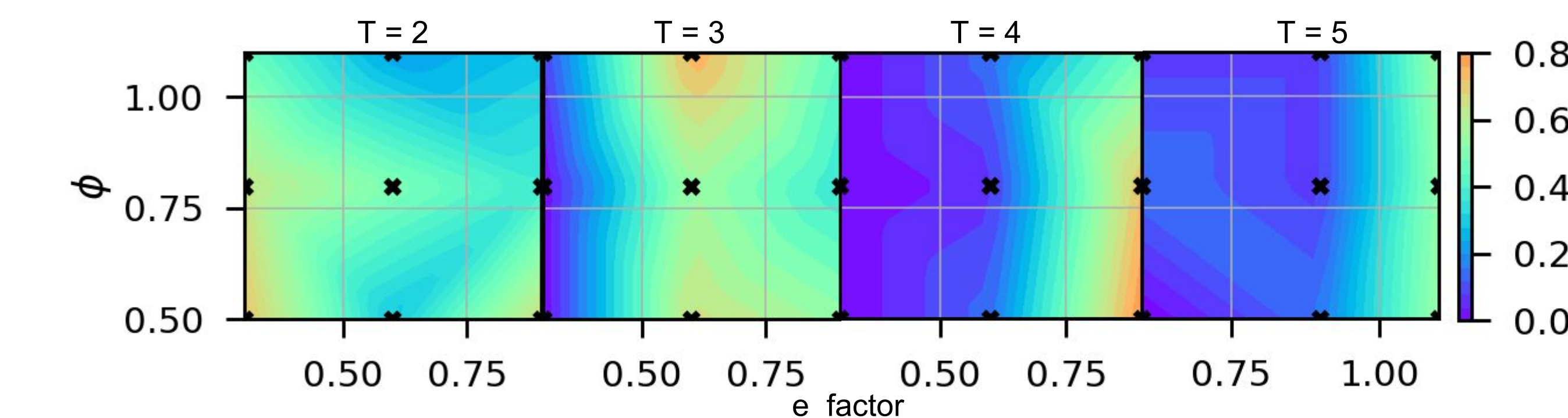


Figure 5: Potential energy over time of sys-A, neither system has definitively reached equilibrium but the difference in behavior is already clear (Left) Disordered with e = 0.3. (Right) Semi-ordered with e = 0.6.

The average P3HT end-to-end distance increases with decreasing ϕ and decreasing e (see Figure 7). This corresponds to a better solvent and lower density which matches our intuition that increasing the space available to molecules and decreasing the strength of their non-bonded interactions will allow them to elongate. The degree of P3HT oligomer stacking correlates with elongation, with stacks unable to form when the oligomer backbones are folded in on themselves.

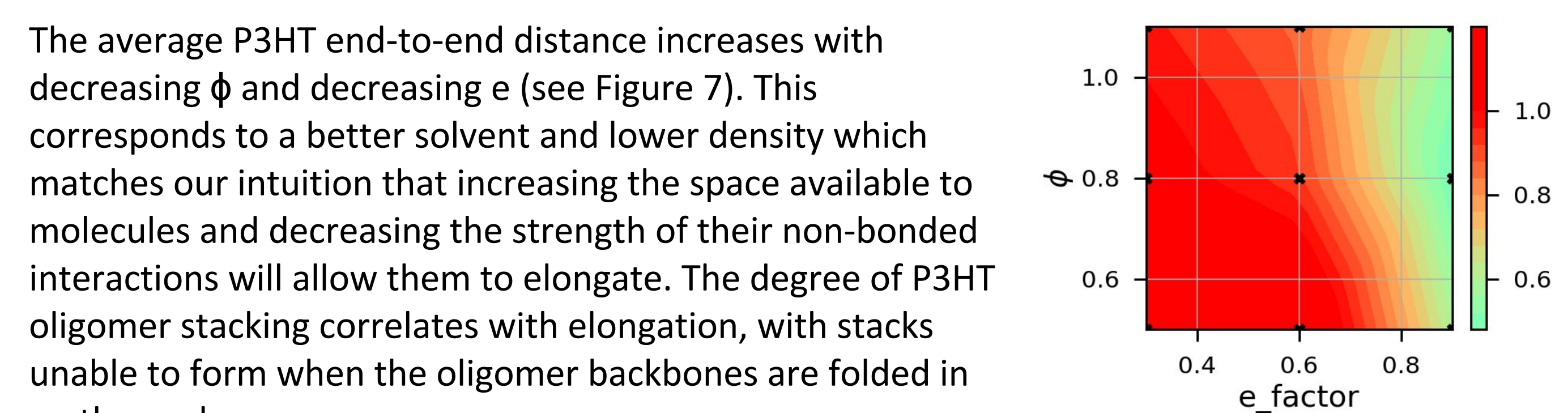


Figure 6: Heat maps depicting the degree of clustering of P3HT in the blend system.

As expected, we find that the morphology of PC₆₁BM and PC₇₁BM blends look qualitatively similar (see Figure 8) due to the similar structure and chemical makeup of the two PCBM variants. However, we expect some quantitative difference due to the different volumes and shapes of the molecules. In Figure 8 we also see evidence of a lamellar stacking phase in the blend systems, although it is much more disordered than that of the neat P3HT system.

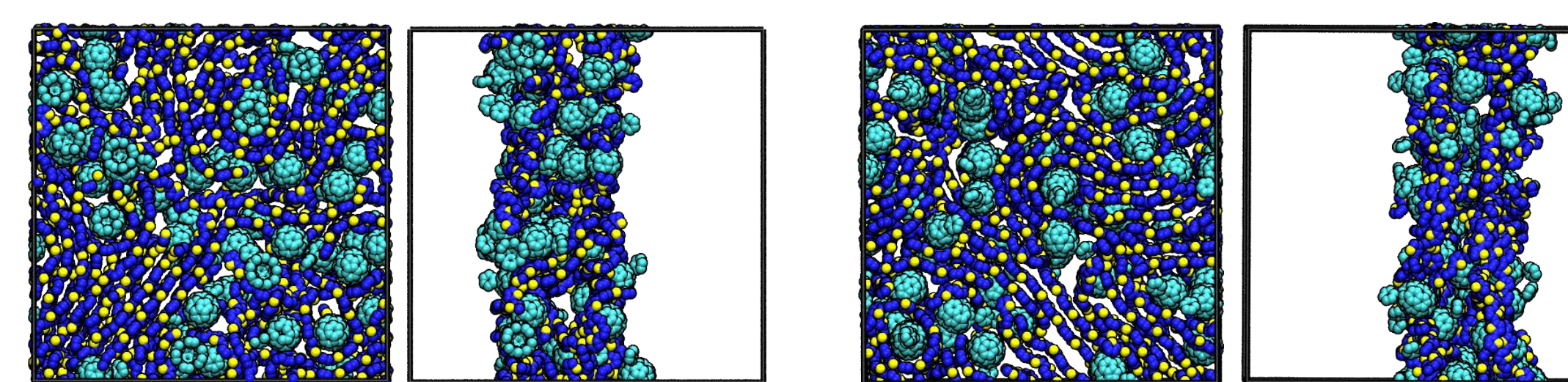


Figure 8: Face-on and side-on view of PC₆₁BM (left) and PC₇₁BM (right) blends at state point T = 4.0, e = 0.9, $\phi = 0.5$.

Results - Neat P3HT

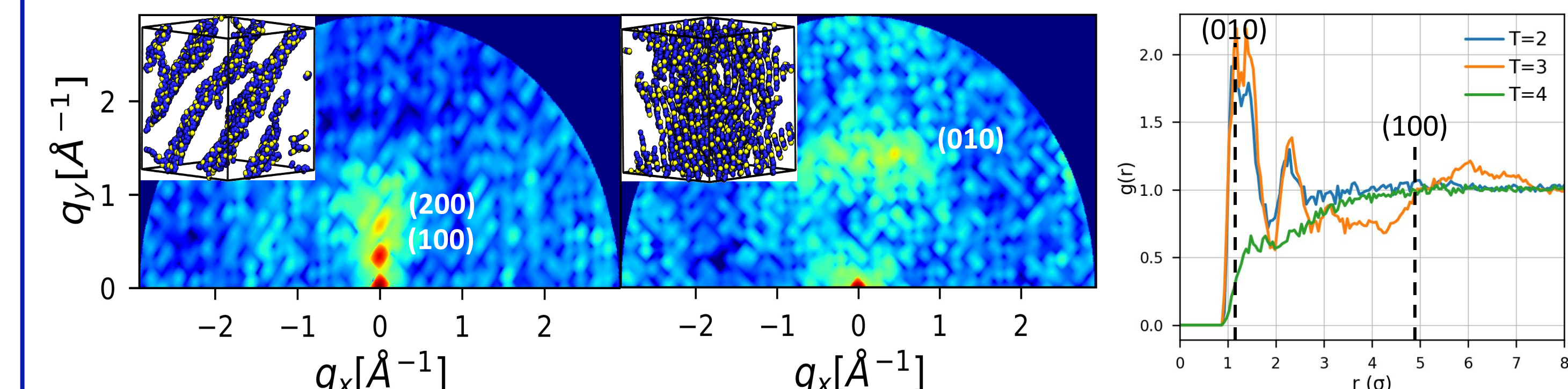


Figure 9: Two different views of simulated GIXS patterns of an ordered neat P3HT system with $\phi = 0.8$ and e = 0.4 (sys-B) at T = 3.0.

In Figure 9 (Right) we again observe the (010) peak from the oligomer stacking. This system also shows a peak (100) corresponding to the space between the lamellae that have formed. Looking at Figure 10, the disordered T = 4 system shows no RDF peaks as expected. In the T = 2 and T = 3 systems which both exhibit π -stacking of P3HT oligomers, we observe a peak between 1σ and 1.5σ , matching the (010) location and a peak around 2.3σ corresponding to the second nearest intrastack neighbor. The T = 3 system has yet another broad peak between 5σ and 7σ representing the distances between the lamellae. The right-shifting of the RDF peaks compared to those from GIXS is likely due to the fact that GIXS uses the smallest gap between the particles of the backbones whereas RDF uses the distance between the thiophene centers of mass.

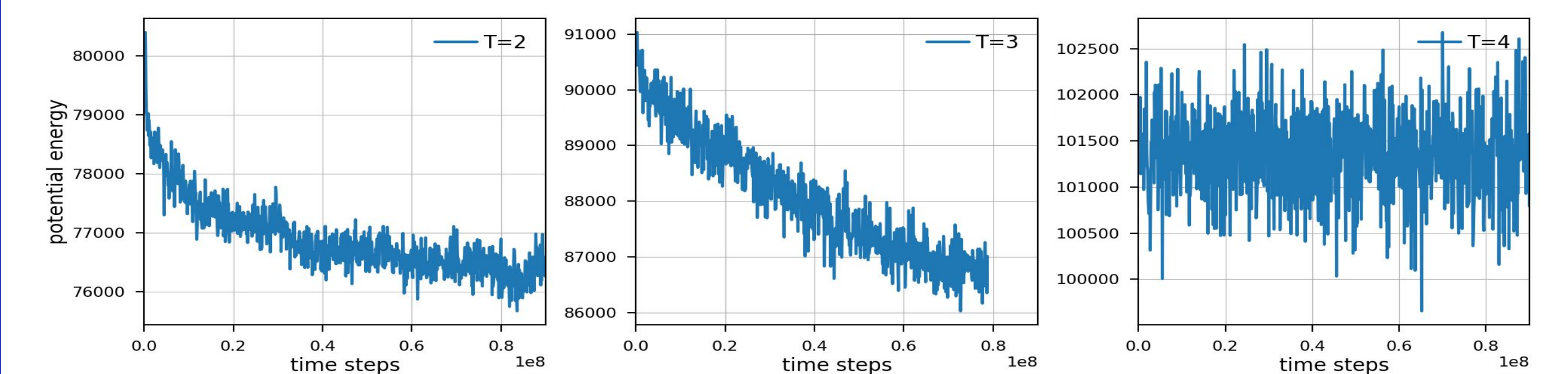


Figure 10: RDF (intra-oligomer exclusion) for sys-B.

The middle potential energy plot corresponds to the lamellar system shown in Figure 9. The linear trend and steeper average slope indicate the more ordered lamellar stacking phase.

Figure 11: Potential as a function of time for the neat P3HT systems at state point $\phi = 0.8$ and e = 0.4. The top plot shows potential energy vs time steps for T = 2, the middle for T = 3, and the bottom for T = 4. The T = 3 plot shows a clear downward trend.

Figure 11: Potential as a function of time for the neat P3HT systems at state point $\phi = 0.8$ and e = 0.4.

The middle potential energy plot corresponds to the lamellar system shown in Figure 9. The linear trend and steeper average slope indicate the more ordered lamellar stacking phase.

Future Work

- **Sampling parameter space at finer intervals**
We were only able to sparsely survey a broad area of phase space in the limited time available. We would gain a better understanding of the various phases by reducing the space between each sample.
- **Running higher throughput simulations**
Many of our systems were run for at most 24 hours and did not reach equilibrium. Additionally, larger systems will yield more realistic results that resemble more closely experimental conditions.
- **Charge transport calculations**
The purpose of this project is to connect device morphology to device efficiency. The next step involves simulating electrons and holes traveling through the morphology and eventually simulating entire devices using these morphologies.
- **Quantitative characterization of difference in two PCBM systems**
The two systems look qualitatively similarly but will likely differ in electronic properties (e.g. charge transport) due to minor differences in ordered morphologies.

Acknowledgement

The authors would like to thank the National Science Foundation for funding this project, Boise State University for hosting the REU program, and all the members of the CME lab, especially Dr. Eric Jankowski, Dr. Matthew Jones, Evan Miller, Stephen Thomas, and Mike Henry for their endless wisdom and unwavering support.

References:

- ¹Jones, M. L. and Jankowski, E. Computationally Connecting Organic Photovoltaic Performance to Atomistic Arrangements and Bulk Morphology *Molecular Simulation* 43(10-11): 756-773. March 2017. <http://dx.doi.org/10.1080/08927022.2017.1296958>
- ²Effects of Thermal Annealing On the Morphology of Polymer-Fullerene Blends for Organic Solar Cells <https://www.ssrli.stanford.edu/content/science/highlight/>; January 31, 2011.
- ³J. A. Anderson, C. D. Lorenz, and A. Travesset. General purpose molecular dynamics simulations fully implemented on graphics processing units *Journal of Computational Physics* 227(10): 5342-5359, May 2008. [10.1016/j.jcp.2008.01.047](https://doi.org/10.1016/j.jcp.2008.01.047)
- ⁴J. Glaser, T. D. Nguyen, J. A. Anderson, P. Liu, F. Spiga, J. A. Millan, D. C. Morse, S. C. Glotzer. Strong scaling of general-purpose molecular dynamics simulations on GPUs *Computer Physics Communications* 192: 97-107, July 2015. [10.1016/j.cpc.2015.02.028](https://doi.org/10.1016/j.cpc.2015.02.028)
- ⁵R. T. McGibbon, K. A. Beauchamp, M. P. Harrigan, C. Klein, J. M. Swails, C. X. Hernandez, C. R. Schwantes, L-P. Wang, T. J. Lane, V. S. Pande. MDTraj: A Modern Open Library for the Analysis of Molecular Dynamics Trajectories *Biophysical Journal* 109(8): 1528-1532, 2015. [10.1016/j.bpj.2015.08.015](https://doi.org/10.1016/j.bpj.2015.08.015)